DOPING EFFECT OF WO_3 ON THE STRUCTURE AND LUMINESCENT PROPERTIES OF $ZnO\text{-}B_2O_3\text{-}Bi_2O_3:Eu^{3+}$ GLASS

Lyubomir Aleksandrov[1], Aneliya Yordanova[1],
Margarita Milanova[1], Reni Iordanova[1], Margit Fabian[2]

[1]*Institute of General and Inorganic Chemistry*
Bulgarian Academy of Sciences, 11 G. Bonchev str.
1113 Sofia, Bulgaria
[2]*Centre for Energy Research, Konkoly Thege Street 29-33*
1121 Budapest, Hungary
E-mail: lubomirivov@gmail.com

Received 03 February 2023
Accepted 09 March 2023

ABSTRACT

In this study we have investigated the effect of the addition of WO_3 to the Eu^{3+}-doped $50ZnO:40B_2O_3:10Bi_2O_3$ glass on its structure and physical properties (density, molar volume, glass transition temperature) by using IR spectroscopy, density measurement and DCS analysis. IR revealed that the inclusion of small amount WO_3 modify borate network, favoring formation of high number of BO_3 units with non-bridging oxygens as a results of the destruction of BO_4 containing superstructural units ($BO_4 \rightarrow BO_3$ transformation). Tungstate ions incorporate into base zinc-bismuth-borate glass as octahedral $[WO_4O_2]^{2-}$ species with four bridging and two non-bridging oxygen atoms. The PL emission spectra at room temperature of the prepared materials were measured. The observed slight increase of the emission intensity of the rare earth Eu^{3+} ion in the spectrum of WO_3 containing glass is an indication of the occurrence of non-radiative energy transfer from glass host to the active ion. The most intense luminescence peak observed at 612 nm suggest that the glasses are potential materials for red emission.

Keywords: *glass structure, DSC, luminescence properties.*

INTRODUCTION

The design of new glass compositions remains a very active field of research due to their exciting application possibilities and the ability to fabricate them in larger scale with lower production cost. For example, glasses are key materials for development of lasers and optoelectronic devises. In particular, glasses doped with trivalent europium ions (Eu^{3+}) are commonly used as red emitting materials for field emission technology and LEDs because of the intense red Eu^{3+} emission at 612 nm ($^5D_0 \rightarrow {}^7F_2$ transition). As the luminescent properties of Eu^{3+} ions strongly depend on the chemical composition and structure of host glass matrix, searching for a suitable Eu^{3+} glass matrix is of a paramount importance for achieving high intensity fluorescence and high brightness [1]. Among many potential host glass materials, the ternary zinc bismuth borate glasses - $ZnO\text{-}B_2O_3\text{-}Bi_2O_3$ have been attracting scientific interest as a host for luminescence applications as they possess low melting temperature, large refractive index, good physical and chemical properties [2 - 6]. Zinc bismuth borate glasses doped with different Eu^{3+} concentrations (1, 3, 5, 7 and 9 mol %) were prepared and their red emitting efficiencies were studied for the development of phosphors device [5]. For all the studied glasses, the strongest peak was found at 613 nm (red emission). The decay time curve exhibited a single exponential nature for all the glasses and the measured decay time was found to decrease with the increase of Eu^{3+} concentration. Systematic analysis of the results suggested that the glass doped with Eu^{3+} concentration near 5 mol % is suitable for LED and display device applications.

From the literature, it is evident that the addition of WO_3 to different tellurite, borate and phosphate glasses strongly improves their thermal, physical and optical

properties [7, 8]. Due the high polarizability, WO_3 could contribute in a great extent to the obtaining of high refractive index glasses and enhanced non-linear optical properties and improved luminescent properties of RE ions [9, 10]. In our recent paper, we have reported for the efficiency of the $50ZnO:40B_2O_3:10WO_3$ glass composition as host matrix for Eu^{3+} ions [11]. It has been established that the addition of WO_3 suppresses the phase separation of the zinc-borate glass at high rare earth doping concentrations and improves Eu^{3+} luminescence emission. The most intense luminescence peak observed at 612 nm and the high-integrated emission intensity ratio (R) of the $^5D_0 \rightarrow {}^7F_2/{}^5D_0 \rightarrow {}^7F_1$ transitions at 612 and 590 nm of 5.77 suggest that the glasses are potential materials for red emission. Motivated by these results, in this work we investigate the doping effect of WO_3 on the structure and luminescent properties of Eu^{3+} doped $ZnO\text{-}B_2O_3\text{-}Bi_2O_3$ glass by using of IR spectroscopy, density measurements and photoluminescent spectroscopy. The aim is to gain a structural information and to check its possible use for visible red emission application.

EXPERIMENTAL

Two glass samples (without and containing 0.5 mol % WO_3) with the chemical composition in mol % of $50ZnO:(40\text{-}x)B_2O_3:10Bi_2O_3:0.5Eu_2O_3:xWO_3$, x = 0 and 0.5 were obtained by applying the conventional melt-quenching method. All specimens were prepared using commercial powders of reagent grade WO_3, ZnO, H_3BO_3, and Eu_2O_3 as starting materials. The homogenized batches were melted at 1200°C for 20 min in a platinum crucible in air. The melts were cast into graphite molds to get bulk samples. The amorphous state of the samples was confirmed by X-ray diffraction analysis (XRD) with a Bruker D8 Advance diffractometer, using Cu K_α radiation in the $10 < 2\Theta < 60$ range, and scanning electron microscopy studies (SEM). SEM/EDX measurements were performed (5 kV, 30 kV) using a Thermo Scientific Scios2 dual beam microscope, Oxford X-maxn 20 SDD EDX. The glass transition (T_g) and crystallization (T_c) temperatures of the glasses were determined using differential scanning calorimetry (DSC 404 F3 Pegasus, NETZSCH, Germany). The heating rate was 10K/min in helium atmosphere under airflow of 30 mL/min. The density of the obtained glasses at room temperature was estimated by Archimedes principle using toluene ($\rho = 0.867$ g/cm^3) as an immersion liquid on a Mettler Toledo electronic balance of sensitivity 10^{-4} g. From the experimentally evaluated density values the molar volume (V_m), the molar volume of oxygen (V_o) (volume of glass in which 1 mol of oxygen is contained) and the oxygen packing density (OPD) of glasses obtained were estimated, using the following relations respectively:

$$V_m = \frac{\Sigma x_i M_i}{\rho_g} \quad (1)$$

$$V_o = V_m \times \left(\frac{1}{\Sigma x_i n_i}\right) \quad (2)$$

$$OPD = 1000 \times C \times \left(\frac{\rho_g}{M}\right) \quad (3)$$

where x_i is the molar fraction of each component i, M_i is the molecular mass, ρ_g the glass density and n_i is the number of oxygen atoms in each oxide, C is the number of oxygen per formula units, and M is the total molecular mass of the glass compositions. The IR spectra of the obtained samples were measured using the KBr pellet technique on a Nicolet-320 FTIR spectrometer with a resolution of ± 4 cm^{-1}, by collecting 64 scans in the range 1600 cm^{-1} - 400 cm^{-1}. A random error in the center of IR bands was found as ± 3 cm^{-1}. Emission spectra at room temperature were measured with a high-resolution spectrometer (Ocean Insight HR 2000+), using a UV LED light sources at 385 nm.

RESULTS AND DISCUSSION

XRD spectra, DSC and scanning electron microscopy studies

Bulk, transparent glasses, with dark brownish coloration were obtained and their X-ray diffraction patterns are shown on Fig. 1. The absence of sharp peaks in the X-ray diffraction spectra showed that prepared samples are glassy in nature. The SEM micrographs of investigated glasses are shown in Fig. 2(a), (x = 0), and 3(a), (x = 0.5). Both images were found to be similar and they suggest the glassy nature of the sample as exhibit a surface without any presence microstructure (grains or grain boundaries). The EDX elemental mapping in Figs. 2(b), (c), (d), (e), (f), (g) and Figs. 3(b), (c), (d), (e), (f), (g), (h) revealed that Zn, B, O, Bi, Eu and W elements are uniformly distributed in

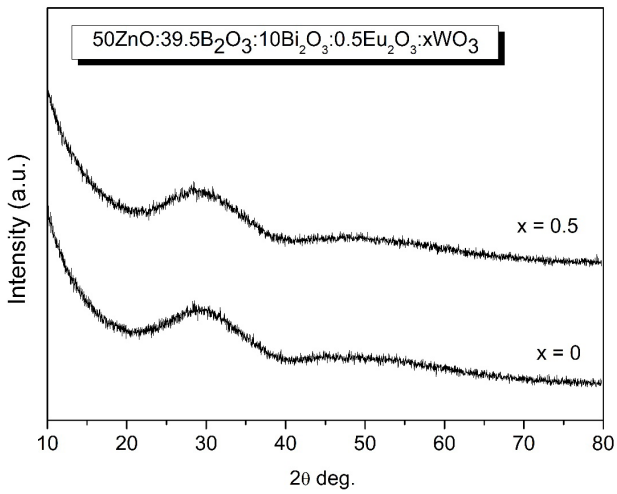

Fig. 1. XRD patterns of glasses $50ZnO:(40-x)B_2O_3:10Bi_2O_3:0.5Eu_2O_3:xWO_3$, x = 0 and 0.5 (in mol. %).

glasses x = 0 and x = 0.5, respectively. The DSC curves for bulk glasses are shown on Fig. 4. Both glasses are characterized with two humps, corresponding to two glass transition temperatures indicated as T_{g1} and T_{g2}, followed by one exothermic effect connected with the crystallization temperatures of the glasses (T_c). The two glass transition effects, observed are due to the presence of two amorphous phases with different compositions in the investigated glasses. The values of T_{g1} and T_{g2} using the onset method and the values of T_c estimated from the exothermic peaks maximum from DSC curves are summarized in Table 1. The thermal stability of glasses

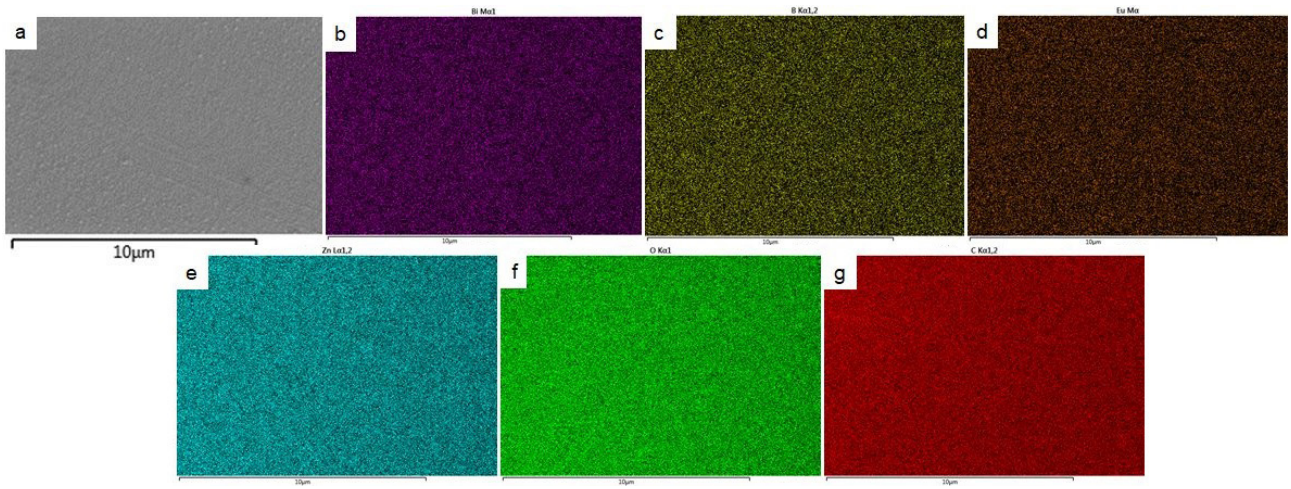

Fig. 2. SEM image (a) and EDX mapping images of Bi (b); B (c); Eu (d); Zn (e); O (f) ; C (g) of glass $50ZnO:40B_2O_3:10Bi_2O_3:0.5Eu_2O_3$.

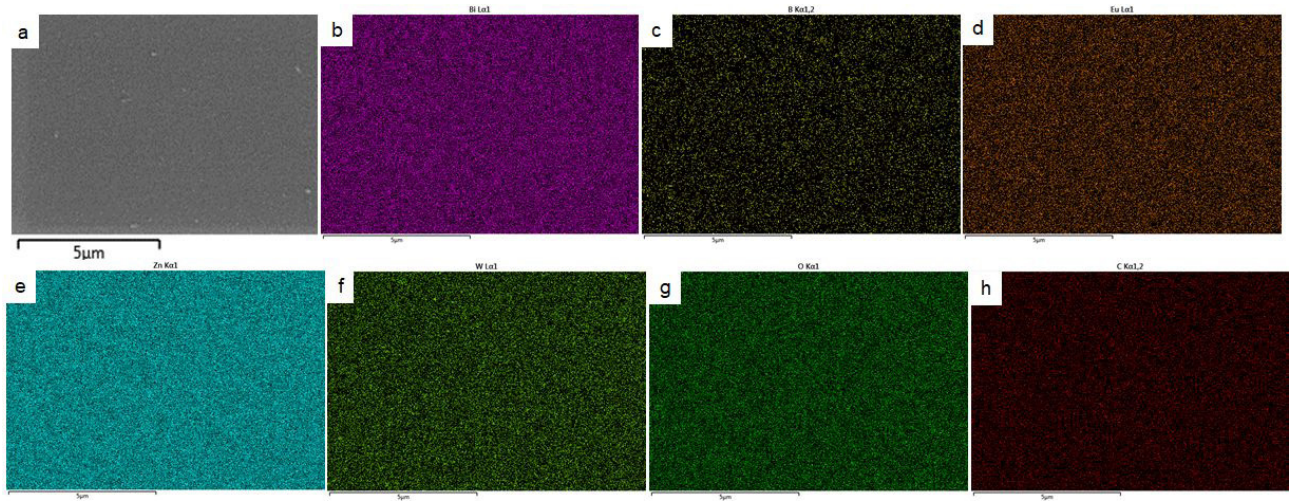

Fig. 3. SEM image (a) and EDX mapping images of Bi (b); B (c); Eu (d); Zn (e); W(f); O (g); C (h) of glass $50ZnO:(40-x)B_2O_3:10Bi_2O_3:0.5Eu_2O_3:0.5WO_3$.

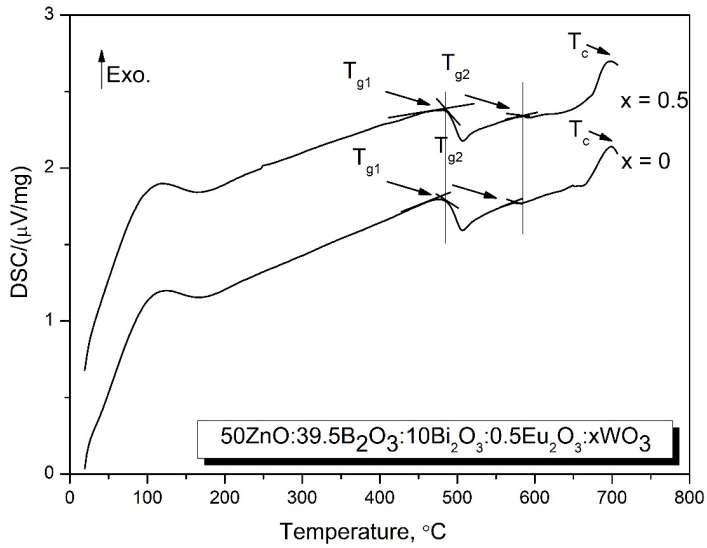

Fig. 4. DTA curves of glasses 50ZnO:(40-x)B_2O_3:10Bi_2O_3:0.5Eu_2O_3:xWO_3, x = 0 and 0.5 (in mol. %).

Table 1. Various physical parameters of 50ZnO:(40-x)B_2O_3:10Bi_2O_3:0.5Eu_2O_3:xWO_3, x = 0 and 0.5 glasses.

Sample ID	ρ (± 0.001 g cm^{-3})	V_m (cm^3 mol^{-1})	V_o (cm^3 mol^{-1})	OPD (g atom/l)	T_{g1} (°C)	T_{g2} (°C)	T_c (°C)	ΔT (°C)
x = 0	5.084	22.99	11.41	87.65	478	574	699	221
x = 0.5	5.105	23.05	11.44	87.42	485	585	699	214

against crystallization, $\Delta T = T_c - T_{g1}$ is also included in the table. As it is seen, the values of all characteristics temperatures for x = 0 and x = 0.5 established do not differ significantly, evidencing that the addition of WO_3 slightly modifies the base glass structure. The obtained glasses are thermally stable as they have a value of ΔT greater than 200°C [12].

IR analysis and physical parameters

The structure of the glasses is studied by IR spectroscopy. The obtained IR glass spectra are shown in Fig. 5. As it is seen from the figure, the IR spectrum of the WO_3-free glass (x = 0) exhibit three distinct absorption profiles situated between 1600 cm^{-1} - 1100 cm^{-1}, 1100 cm^{-1} - 750 cm^{-1} and 750 cm^{-1} - 400 cm^{-1}. The absorption in the range between 1600 cm^{-1} - 1100 cm^{-1} is connected with the stretching vibrations of the B-O bonds in the trigonal BO_3 units. Having in mind the IR bands assignments proposed for similar glass compositions given in refs. [11, 13 - 16], the shoulder at 1460 cm^{-1} and the not well resolved band at 1320 cm^{-1} are ascribed to the stretching vibration of non-bridging B-O^- bonds in metaborate units, BO_2O^- and in pyroborate units, $[B_2O_5]^{4-}$ respectively. Another not well resolved band at about 1280 cm^{-1} has a complex character. It can be connected with the B-O stretch in BO_2O^- groups and as well as with the ν_3 asymmetric stretching vibration of orthoborate triangular units, $[BO_3]^{3-}$ [16]. The shoulder at 1175 cm^{-1} is due to the B-O-B stretch in pyroborate groups, $[B_2O_5]^{4-}$ [16]. The absorption envelope between 1100-750 cm^{-1} contains two weak bands at 1080 cm^{-1} and 1045 cm^{-1} connected with the vibration of the BO_4 tetrahedral units from different superstructural borate groups (tri-, tetra- and pentaborate groups) [14, 15]. The third spectral region between 750 cm^{-1} -400 cm^{-1} displays a shoulder at 670 cm^{-1}, strong band at 620 cm^{-1} and band at 480 cm^{-1}. The shoulder at 670 cm^{-1} is due to the bending vibration of B-O-B bonds in superstructural units containing BO_3 and BO_4 groups [14]. The strong band at 620 cm^{-1} can be assigned to overlapping contributions from the bending vibration of B-O-B bonds in meta- and pyroborates and the vibration of Bi-O bonds in strongly deformed and BiO_6 octahedra [14]. The absorption bands at 480 cm^{-1} is also specific to the vibrations of Bi-O bonds in BiO_6

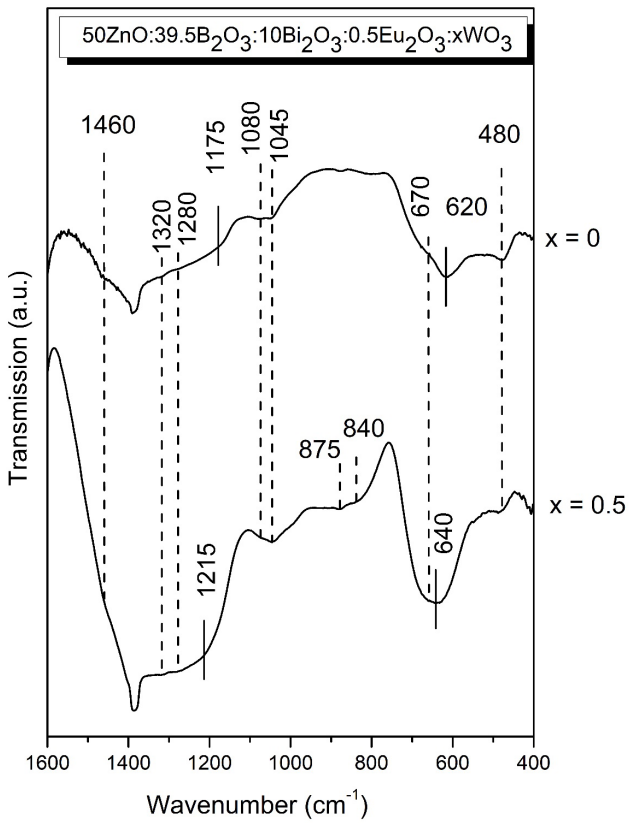

Fig. 5. Infrared spectra of glasses 50ZnO:(40-x) B_2O_3:10Bi_2O_3:0.5Eu_2O_3:xWO_3, x = 0 and 0.5 (in mol. %).

octahedral units [14, 16].

The introduction of 0.5 mol. % WO_3 into glass 50ZnO:40B_2O_3:10Bi_2O_3:0.5Eu_2O_3 causes changes in its vibrational spectrum, which reflect some structural modifications. As one can see from the Fig. 5, the absorption bands in the spectrum of WO_3-containing glass (x = 0.5) are with higher intensity, evidencing decreasing structural disorder in the glass network. The band at 1280 cm^{-1} ($\nu_{3,}$ $[BO_3]^{3-}$) became stronger, and the shoulder at 1175 cm^{-1} (B-O-B bridges in pyroborates) upshifts to 1215 cm^{-1} and increases in intensity as compared, with the glass x = 0. The intensity of the band at 1080 cm^{-1} related with the vibrations of BO_4 from superstructural units, lowers, evidencing decreasing number of these structural groups. These spectral observations evidence that the inclusion of small amount WO_3 modify borate network, favoring formation of high number of BO_3 units with non-bridging oxygens as a results of the destruction of BO_4 containing superstructural units ($BO_4 \rightarrow BO_3$ transformation). In the IR spectrum of glass x = 0.5 new bands at 875 cm^{-1}, 840 cm^{-1} appear, and the shoulder at 670 cm^{-1} turns into a band. Also, the band at 620 cm^{-1} become stronger and upshifts to the 640 cm^{-1}. These spectral changes are connected with the presence of tungstate entities in the glass structure. According to the literature, the IR spectrum of crystalline $ZnWO_4$ with wolframite type structure consisting of octahedral $[WO_4O_2]^{2-}$ species with four bridging and two non-bridging oxygen atoms is characterized with the strong bands at 870 cm^{-1}, 840 cm^{-1}, 685 cm^{-1} 650 cm^{-1} and 530 cm^{-1} [17]. The bands at 870 cm^{-1} and 840 cm^{-1} are ascribed the vibrations of terminal WO_2 units. Lower-frequency bands at 685 cm^{-1}, 650 cm^{-1} and 530 cm^{-1} are associated with $\nu_{as}[W_2O_4]_n$ and $\nu_s[W_2O_4]_n$ vibrations, which involve mainly the W-O_2-W double bridges of the $[W_2O_4]_n$ chain structure. On this base the new bands at 875 cm^{-1} and 840 cm^{-1} in the spectrum of x = 0.5 glass are due to the $\nu_s(WO_2)$ and $\nu_{as}(WO_2)$ vibrations of the WO_2 entities. The two strong bands at 670 cm^{-1} and 640 cm^{-1} are connected with the asymmetric stretching vibrations of two-oxygen bridges (W_2O_2) in octahedral $[WO_4O_2]^2$ species, overlapping with the vibrations of borate oxygen network.

Additional information for the effect of WO_3 on the structure of the base Eu^{3+}-doped zinc - bismuth - borate glass is obtained by comparative analysis of the physical parameters: density(ρ), molar volume (V_m), oxygen molar volume (V_o) and oxygen packing density (OPD) of x = 0 and x = 0.5 glasses, which are listed in Table 1. As it is seen from the table, the WO_3-containing glass (x = 0.5) is characterized with a higher density compared to the WO_3-free glass (x = 0) because of the replacement of lighter B_2O_3 (Mw 69.62 g/mol) with heavier WO_3 (Mw 231.84 g/mol) [18]. Molar volume for x = 0.5 glass is also higher as compared with V_m of glass x = 0 evidencing that the incorporation of WO_3 results in expanding of the glass network. The free volume created is due to the difference of ionic radius between W^{6+} (0.6 Å) and B^{3+} (0.11 Å) [19]. Oxygen molar volume (V_o) and OPD are two parameters that give information for packing of the oxygen ions in the glass structure [20]. Low V_o and high OPD are indication for high degree of network connectivity. The x = 0.5 glass is characterized with higher V_o and lower OPD values compared to those established for x = 0 glass, indicating that the introduction of WO_3 cause an increase in the number of non-bridging oxygens (NBOs) and reduces crosslinking within the glass network [11].

This result is consistent with IR spectral data revealing an accumulation of BO_3 groups with NBOs in the glass structure of Eu^{3+} doped zinc-bismuth-borate glass when WO_3 is added.

Photoluminescence properties

The room temperature photoluminescence spectra of the obtained 0.5 mol. % Eu_2O_3 doped $50ZnO:40B_2O_3:10Bi_2O_3$ and $50ZnO:39.5B_2O_3:10Bi_2O_3$-$0.5WO_3$ glasses are shown in Fig. 6. Under the excitation of 385 nm, the specimens exhibit only intra-configurational transitions of Eu^{3+} ions from $^5D_0$ to ^7F_J (J = 0, 1, 2, 3 and 4) states located at 578 nm, 591 nm, 612 nm, 651 nm and 700 nm, respectively [1]. According to the literature data, the characteristic broad band emission of WO_n groups is observed in the spectral region between 400 nm and 600 nm. In the present case, no emission band in this spectral region is detected at sample doped with 0.5 mol. % WO_3. The observed slight increase of the emission intensity of the rare earth Eu^{3+} ion in the spectrum of WO_3 containing glass is an indication of the occurrence of non-radiative energy transfer from glass host to the active ion [21]. Comparing the characteristic emission peaks of Eu^{3+}, it is clearly observed that the luminescence band originating from the transition $^5D_0 \rightarrow ^7F_2$ is the most intensive one. This result suggests the Eu^{3+} doped glasses can produce red luminescence with high color purity and can be used as potential red - emitting materials. The second most intensive peak is located at 591 nm arising from $^5D_0 \rightarrow ^7F_1$ transition.

It is generally accepted that the hypersensitive electric dipole (ED) transition $^5D_0 \rightarrow ^7F_2$ largely depends on the local symmetry in the surrounding around active ions and usually dominates in the emission spectrum when Eu^{3+} ions are localized at sites with low symmetry, whereas the insensitive magnetic dipole (MD) transition $^5D_0 \rightarrow ^7F_1$ is independent of the local symmetry of coordination environment around Eu^{3+} and is predominant when Eu^{3+} ions occupy the inversion symmetry sites [1, 22 - 24]. In the present case, the fact that the dominant emission is from the ED transition rather than from the MD transition indicates, that Eu^{3+} ions are situated at sites with non-inversion symmetry. Furthermore, the integrated emission intensity ratio (R) of these two transitions ($^5D_0 \rightarrow ^7F_2/^5D_0 \rightarrow ^7F_1$) is used as a spectroscopic key to estimate the degree of asymmetry of the coordination environment around Eu^{3+} ions and to determine the strength of covalent bonding between Eu^{3+} ion and its surrounding ligand anions [1, 25, 26]. The higher ratio values correspond to a more distorted (asymmetric) local environment around the active ion site, stronger Eu-O covalence and more intensive luminescence. The calculated R values (3.58 and 3.79) of the prepared glasses are in the same range with the other reported in the literature Eu^{3+} doped oxide glasses (Table 2), [27 - 31]. On the other hand, these values are found

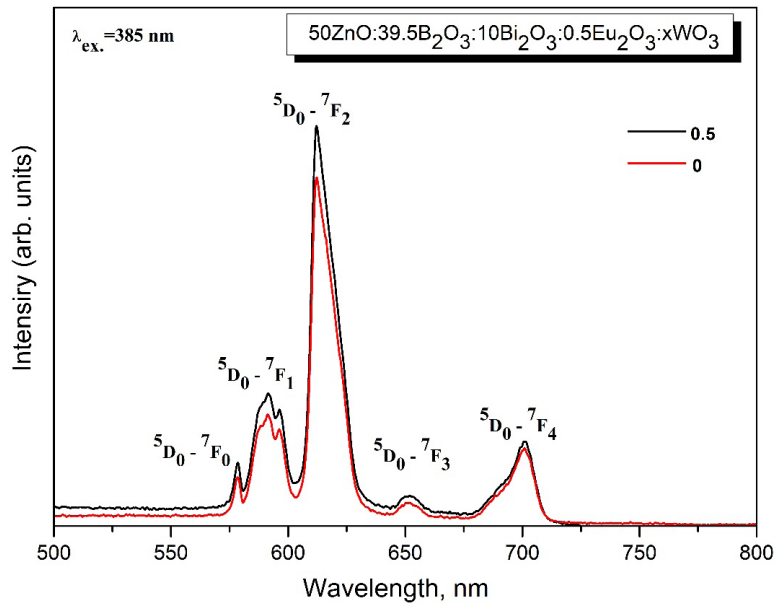

Fig. 6. Emission spectra of glasses $50ZnO:(40-x)B_2O_3:10Bi_2O_3:0.5Eu_2O_3:xWO_3$, x = 0 and 0.5 (in mol. %).

Table 2. Fluorescence intensity ratio (R) of 50ZnO:(40-x)B_2O_3:10Bi_2O_3:0.5Eu_2O_3:xWO_3, (x = 0 and 0.5 mol. %) glasses and other Eu^{3+} ion doped oxide glasses.

Glass composition	Fluorescence intensity ratio, R	References
50ZnO-40B_2O_3-10Bi_2O_3-0.5Eu_2O_3	3.58	Present work
50ZnO-39.5B_2O_3-10Bi_2O_3-0.5Eu_2O_3-0.5WO_3	3.79	Present work
50ZnO-40B_2O_3-10WO_3-xEu_2O_3 ($0 \le x \le 10$)	4. 54 - 5.77	11
0.01Eu_2O_3.0.99(25Na_2O-50B_2O_3-25SiO_2)	3.33	27
(40-x) B_2O_3-15TeO_2-15Li_2CO_3-15LiF-15NaF-xEu_2O_3, (where x = 0.05, 0.1, 0.25, 0.5, 1 and 2 wt%)	2.82 - 4.54	28
4ZnO-3B_2O_3.0.5 ÷ 2.5 mol % Eu^{3+}	2.74 - 3.94	29
60TeO_2-19ZnO-7.5Na_2O-7.5Li_2O-5Nb_2O_5-1Eu_2O_3	3.73	30
Eu^{3+}: 45B_2O_3-5ZnO-49PbO	3.03	31

to be lower compared to the previously studied by us 50ZnO:40B_2O_3:10WO_3:xEu_2O_3 ($0 \le x \le 10$) glasses [11]. This result indicates formation of a more symmetrical amorphous network in the obtained glasses, probably due to the presence of Bi_2O_3. The obtained close R values (3.58 and 3.79) are an indication of the local environment similarity for both glasses. The higher emission intensity of WO_3 containing glass is a proof that the non-radiative energy transfer from WO_n to the Eu^{3+} ions has a greater impact on the emission intensity, rather that the local symmetry environment around active ions.

CONCLUSIONS

The doping effect of WO_3 on the structure and luminescent properties of Eu^{3+} doped ZnO-B_2O_3-Bi_2O_3 glass was investigated. The synthesized amorphous networks are built up of metaborate, $[BO_2O]^-$, pyroborate, $[B_2O_5]^{4-}$, orthoborate triangular units, $[BO_3]^{3-}$ and octahedral $[WO_4O_2]^{2-}$ species with four bridging and two non-bridging oxygens. Bismuth atoms participate as BiO_6 groups. WO_3 modify borate network, causing $BO_4 \rightarrow BO_3$ transformation and as a result formation of high number of BO_3 units with non-bridging oxygens. The positive effect of WO_3 on the luminescence intensity of the Eu^{3+} doped zinc borate glass was established.

Acknowledgements

This work is supported by joint research project within the framework of an international scientific cooperation between BAS and MTA IC-HU/01/2022-2023. Research equipment of the National Centre for Mechatronics and Clean Technologies was used for the experiments (project BG05M2OP001-1.001-0008, funded by the European Regional Development Fund under the Operational Program "Science and Education for Smart Growth 2014-2020").

REFERENCES

1. K. Binnemans, Interpretation of europium (III) spectra, Coord. Chem. Rev., 295, 2015, 1-45.
2. A.D. Sontakke, A. Tarafder, K. Biswas, K. Annapurna, Sensitized red luminescence from Bi^{3+} co-doped Eu^{3+}: ZnO-B_2O_3 glasses, Physica B: Condensed Matter., 404, 20, 2009, 3525-3529.
3. I. Pal, S. Sanghi, A. Agarwal, M.P. Aggarwal, Spectroscopic and structural investigations of Er^{3+} doped zinc bismuth borate glasses, Mater. Chem. Phys., 133, 2012, 153-158.
4. T. Inoue, T. Honma, V. Dimitrov, T. Komatsu, Approach to thermal properties and electronic polarizability from average single bond strength in ZnO–Bi_2O_3–B_2O_3 glasses, J. Solid State Chem., 183, 2010, 3078-3085,
5. J. Kaewkhao, K. Boonin, P. Yasaka, H.J. Kim, Optical and luminescence characteristics of Eu^{3+} doped zinc bismuth borate (ZBB) glasses for red emitting device, Mater. Res. Bull., 71, 2015, 37-41.
6. P. Chimalawong, K. Kirdsiri, J. Kaewkhao, P. Limsuwan, Structural and optical properties of Ho^{3+} doped ZnO-Bi_2O_3-B_2O_3 glasses, Adv. Mater. Res., 979, 2012, 98-101.

7. G. AlMisned, D.S. Baykal, G. Susoy, G. Kilic, H.M.H. Zakaly, A. Ene, H.O. Tekin, Determination of gamma-ray transmission factors of WO_3-TeO_2-B_2O_3 glasses using MCNPX Monte Carlo code for shielding and protection purposes, Applied Rheology, 32, 2022, 166-177.
8. M. Ataalla, A.S. Afify, M. Hassan, M. Abdallah, Margarita Milanova, H.Y. Aboul-Enein, A. Mohamed, Tungsten-based glasses for photochromic, electrochromic, gas sensors, and related applications: A review, J. Non-Cryst. Solids, 491, 2018, 43-54.
9. D. Munoz-Martín, M.A. Villegas, J. Gonzalo, J.M. Fernández-Navarro, Characterization of glasses in the TeO_2–WO_3–PbO system, J. Eur. Ceram. Soc., 29, 2009, 2903-2913.
10. M. Reza Dousti, G.Y. Poirier, A. Simone Stucchide Camargo, Structural and spectroscopic characteristics of Eu^{3+}-doped tungsten phosphate glasses, Opt. Mater., 45, 2015, 185-190.
11. M. Milanova, L. Aleksandrov, A. Yordanova, R. Iordanova, N.S. Tagiara, A. Herrmann, G. Gao, L. Wondraczek, E.I. Kamitsos, Structural and luminescence behavior of Eu^{3+} ions in ZnO-B_2O_3-WO_3 glasses, J. Non-Cryst. Solids, 600, 2023, 122006.
12. S. Patel, B. Fageria, K.S. Gill, S. Soni , V.N. Mishra, Thermal and structural properties of ZnO-Bi_2O_3-B_2O_3 glasses doped with NiO, Eurasian J. Phys. Funct. Mater., 6, 1, 2022, 85-92.
13. R. Iordanova, M. Milanova, L. Aleksandrov, K. Shinozaki, T. Komatsu, Structural study of WO_3-La_2O_3-B_2O_3-Nb_2O_5 glasses, J. Non-Cryst. Solids, 543, 2020, 120132.
14. R. Iordanova, M. Milanova, L. Aleksandrov, A. Khanna, Structural study of glasses in the system B_2O_3-Bi_2O_3-La_2O_3-WO_3, J. Non-Cryst. Solids, 481, 2018, 254-259.
15. E.I. Kamitsos, M.A. Karakasides, G.D. Chryssikos, Vibrational Spetcra of Magnesium-Sodium-Borate Glasses. 2. Raman and Mid-Infrared Infestation of the Network Structure, J. Phys. Chem., 91, 1987, 1073-1079.
16. C.P.E. Varsamis, N. Makris, C. Valvi, E.I. Kamitsos, Phys. Chem. Chem. Phys., 23, 2021, 10006.
17. M. Mancheva, R. Iordanova, Y. Dimitriev, Mechanochemical synthesis of nanocrystalline $ZnWO_4$ at room temperature. J Alloys Compd., 509, 2011, 15-20.
18. A. Bajaj, A. Khanna, N.K. Kulkarni, S.K. Aggarwal, Effects of Doping Trivalent Ions in Bismuth Borate Glasses, J. Am. Ceram. Soc., 92, 2009, 1036-1041.
19. Y. Al-Haadethi, M.I. Sayyed, J. Kaewkhao, B.M. Raffah, R. Almalki, R. Rajaramakrishna, M.A. Hussein, Physical, optical properties and radiation shielding studies of xLa_2O_3-(100-x)B_2O_3 glass system, Ceram. Int., 46, 2020, 5380-5386.
20. M.A. Villegas, J.M. Fernández Navarro, Physical and structural properties of glasses in the TeO_2–TiO_2–Nb_2O_5 system, J. Eur. Ceram. Soc., 27, 2007, 2715-2723.
21. P.S. Dutta, A. Khanna, Eu^{3+} Activated Molybdate and Tungstate Based Red Phosphors with Charge Transfer Band in Blue Region, ECS J. Solid State Sci Technol., 2, 2013, R3153-R3167.
22. G. Blasse, B.C. Grabmaier, Luminescent Materials, Springer, VerJag Berlin Heidelberg, 1994, 18.
23. Y. Gandhi, I.V. Kityk, M.G. Brik, P. Raghav Rao, N. Veeraiah, Influence of tungsten on the emission features of Nd^{3+}, Sm^{3+} and Eu^{3+} ions in ZnF_2-WO_3-TeO_2 glasses, J. Alloys Compd., 508, 2010, 278-291.
24. K. Mariselvam, Juncheng Liu, Synthesis and luminescence properties of Eu^{3+} doped potassium titano telluroborate (KTTB) glasses for red laser applications, J. Lumin., 230, 2021, 117735.
25. C.H.B. Annapurna Devi, Sk. Mahamuda, K. Swapna, M. Venkateswarlu, A. Srinivasa Rao, G. Vijaya Prakash, Compositional dependence of red luminescence from Eu^{3+} ions doped single and mixed alkali fluoro tungsten tellurite glasses, Opt. Mater., 73, 2017, 260-267.
26. M. Nogami, N. Umehara, T. Hayakawa, Effect of hydroxyl bonds on persistent spectral hole burning in Eu^{3+} doped BaO-P_2O_5 glasses, Phys. Rev. B., 58, 1998, 6166-6171.
27. D.G. Barton, M. Shtein, R.D. Wilson, S.L. Soled, E. Iglesia, Structure and electronic properties of solid acids based on tungsten oxide nanostructures, J. Phys. Chem. B, 103, 1999, 630-640.
28. R. Vijayakumar, K. Maheshvaran, V. Sudarsan, K. Marimuthu, Concentration dependent luminescence studies on Eu^{3+} doped telluro fluoroborate glasses, Journal of luminescence, 154, 2004, 160-167.
29. M. Bettinelli, A. Speghini, M. Ferrari, M. Montagna,

Spectroscopic investigation of zinc borate glasses doped with trivalent europium ions, J. Non-Cryst. Solids, 201, 1996, 211-221.

30. S. Surendra Babu, Kiwan Jang, Eun Jin Cho, Hoseop Lee, C.K. Jayasankar, Thermal, structural and optical properties of Eu^{3+}-doped zinc-tellurite glasses, J. Phys. D: Appl. Phys., 40, 2007, 5767.
31. G. Lakshminarayana, S. Buddhudu, Spectral analysis of Eu^{3+} and Tb^{3+}:B_2O_3-ZnO-PbO glasses, Mater. Chem. Phys., 102, 2007, 181-186.